New Scandium (III) Coordination Polymers at Bulk and Nano-scale, Synthesis, Characterization, Thermal and Gas sensing Properties

Abedin Zebardasti[۱], Saeid Farhadi[۱], Veysel. T. YILMAZ[۲] and Alireza Aslani[۱]*

Abstract

New Scandium(III) coordination polymer at bulk and nanopowders as Scandium ۱،٤-benzene dicarboxylic acid hydroxide $[Sc(OH)(BDCA)]_n$, (BDCA = ۱،٤-Benzene Dicarboxylic Acid) has been synthesized by the reaction of a mixture Sc(III) Nitrate and BDCA in MeOH by simple Branched tube and sonochemical method. The nanopowders of Sc_2O_3 was prepared from the calcinations of the NCP at air atmosphere. The structure of the CP and NCP (CP = Coordination Polymers and NCP = Nano Coordination Polymers) were determined by X-ray crystallography, while nano-structural materials were characterized by X-ray powder diffraction (XRPD), Thermal Gravimetric Analysis (TGA) and Scanning Electron Microscopy (SEM). These NCP and Sc_2O_3 nanostructures have been tested for CO_2 gas monitoring by depositing them as thick films on an interdigitated alumina substrate and evaluating the surface resistance of the deposited layer as a function of operating temperature and CO_2 concentrations. The gas sensitivity tests have demonstrated that the Sc_2O_3 nanopowders, exhibit high sensitivity to CO_2 proving their applicability in gas sensors. The role of the nanopowdesr on the sensing properties of NCP and Sc_2O_3 are also discussed.

Keywords: Coordination Polymers, Sc_2O_3, Nanopowders, CO_2, gas sensing.

Introduction

A coordination polymer is defined as a polymeric substance containing a coordination compound or metal complex in its repeating unit. The metal complex is not necessarily part of the polymer backbone. Fifteen to twenty years ago, the main interest in coordination polymers depended on the expectation of increased thermal stability for the materials. However as shown by more recent studies, many earlier problems have been overcome, and new, unanticipated application have been realized. In the last decade coordination compounds with infinite one-, two- and three-dimensional network structures have been intensively studied in particular compounds with back-bonds constructed by metal ions and ligand form a family of polymers, which are called "Coordination Polymer" [۱]. Research in the coordination polymers has rapidly grown in recent years due to an increasing demand for functional materials with conducting, magnetic , nonlinear optical, porous, thermal, fluorescence properties [۲].

On the other hand nano-materials are at the leading edge of rapidly developing field of nanotechnology [۳-٦]. A reduction in particle size to nanometer scale results in various special and interesting properties compared to their bulk properties. Metallic nanopowders, specifically materials with Nano-scale features, have been the subject of numerous research efforts in fields such as gas sensors [۷ and ۸], fuel cells [۹], solar cells [۱۰ and ۱۱] and electrodes for lithium ion batteries [۱۲] to name a few. A reduction in particle

۱ Department of Chemistry, University of Lorestan, Lorestan-Khoramabad ۶۸۱۳۵-۴۶۵, Iran, a.aslani۱۱۰@yahoo.com, nanochemistry@yahoo.com. *Corresponding author (Email: a.aslani@sciknow.org)

۲ Department of Chemistry, Faculty of Arts and Sciences, Uludag University, ۱۶۰۵۹ Bursa, Turkey

size to nanometer scale results in various special and interesting properties compared to their bulk properties. Metal oxide materials, specifically materials with nanoscale features, have been the subject of numerous research efforts in fields such as gas sensors [۱۳, ۱٤], fuel cells [۱٥], solar cells [۱٦, ۱۷] and electrodes for lithium ion batteries [۱۸] to name a few. Fan et al. [۱۹] reported oxygen adsorption on the nanowire surface. It was shown a considerable variation of electrical properties of the single crystal $Sc_۲O_۳$ nanowire upon oxygen introduction. Furthermore an interesting study of the response to oxygen as a function of the nanowire dimensions was reported, evidencing an increase in the response as the nanowire radius decreases.

Nevertheless the presented experiments show good sensing properties, the possibility to use dopants and catalyzing such in the thin film gas sensors and the real integration in low power consumption transducers of single crystalline nanopowders. The integration of top down and bottom up approaches prove the feasibility of large scale manufacturing of well-organized sensor arrays based on different nanostructures. The above mentioned Methods cannot be departed from complex chemical reactions or processes. Thermal oxidation may assist the production of catalysts, semiconductor devices or functional oxide films under controlled conditions. A direct and simple thermal oxidation method was employed to synthesize $Sc_۲O_۳$ nanopowders. Using this convenient route, with no catalyst and template assisted, many research teams prepared $Sc_۲O_۳$ nanopowders successfully by oxidizing NCP (Nano Coordination Polymers) of $Sc(OH)[BDCA]_n$ under air conditions respectively. Single Crystal X-Ray analysis, X-Ray diffraction Powder (XRDP), Scanning Electron Microscopy (SEM) and Thermal Gravimetric and Different Thermal Analysis (TGA/DTA) were used to characterize the morphology, structure and phase of the synthesized CP and NCP. In the present work we report data about their gas-sensing properties, by using them as active layers in $CO_۲$ gas resistive sensors. The gas sensing properties of the NCP and $Sc_۲O_۳$ nanostructures were compared and discussed as a function of the morphology of the primary nanoparticles. The results presented highlighted the role of the shape of the primary $Sc_۲O_۳$ crystallites and an explanation based on the characterization and sensing data acquired has been given.

Experimental

Materials and suppliers

All reagents and solvents for the synthesis and analysis in this work, were commercially available and were used as received. A multiwave ultrasonic generator (Bandlin Sonopuls Gerate-Typ: UW ۳۲۰۰, Germany), equipped with a converter/transducer and titanium oscillator (horn), ۱۲,٥ mm in diameter, operating at ۲٤ kHz with a maximum power output of ٦۰۰ W, was used for the ultrasonic irradiation. The ultrasonic generator automatically adjusts the power level. IR spectra were recorded using Perkin-Elmer ٥۹۷ and Nicolet ٥۱۰P spectrophotometers. The DTA and TGA data were obtained using a PL-STA ۱٥۰۰ apparatus and platinum crucibles with a heating rate of ٥ $^{o}Cmin^{-۱}$ in a vacuum. X-Ray Powder Diffraction (XRPD) measurements were performed using a Philips Diffractometer manufactured by X'pert with monochromatized CuK_{α} radiation. Simulated XRPD patterns were calculated using Mercury [۲۰] based on the single crystal data. Particle sizes of selected samples were estimated using the Sherrer method. The samples were characterized with a scanning electron microscope (SEM) (Philips XL ۳۰) with gold coating.

Synthesis

To isolate single crystals of this Coordination-Polymer, BTCA (۰,۱۸٦ g, ۱,۰ mmol) and Sc(III) Nitrate (۰,۲۳۱ g, ۱,۰ mmol) were placed in the main arm of a branched tube. Methanol (MeOH) was carefully

added to fill both arms. The tube was sealed and the ligand-containing arm immersed in an oil bath at ٦٥ ºC while the other arm was kept at ambient temperature. After ٤ days, colorless crystals that deposited in the cooler arm were isolated, filtered off, washed with acetone and ether and air dried. In order to prepare nanopowders, ١٥ ml MeOH solution of Sc(III) nitrate (٠,٣ M) in a vessel was positioned in a high-density ultrasonic probe, operating at ٢٤ kHz with a maximum power output of ٦٠٠ W. Into this solution ١٥ ml solution of the (BTCA) (٠,٣ M) was added drop wise. The precipitates were filtered off, washed with Acetone/Deionized water and then dried in air. The different concentrations of metal and ligand solution (٠,٠٢٥, ٠,٠٥ and ٠,١ M) with the same aging time (١h) were tested at different power of ultrasonic irradiation (٦٠, ١٢٠ and ١٨٠ kHz).

Crystallography

For the crystal structure determination, the single-crystal of the compound was used for data collection on a four-circle Rigaku R-AXIS RAPID-S diffractometer (equipped with a two-dimensional area IP detector). The graphite-monochromatized Mo K_α radiation (λ = ٠,٧١٠٧٣ Å) and oscillation scans technique with $\Delta\omega = ٥^\circ$ for one image were used for data collection. The lattice parameters were determined by the least-squares methods on the basis of all reflections with $F^٢ > ٢\sigma(F^٢)$. Integration of the intensities, correction for Lorentz and polarization effects and cell refinement was performed using Crystal Clear (Rigaku/MSC Inc., ٢٠٠٥) software [٢٠]. The structures were solved by direct methods using SHELXS-٩٧ and refined by a full-matrix least-squares procedure using the program SHELXL-٩٧ [٢١]. The final difference Fourier maps showed no peaks of chemical significance. Details of crystal data, data collection, structure solution and refinement are given in supplementary informations.

Sensing tests

Sensors were made by depositing by drop coating films (١–١٠ μm thick) of the nanopowders dispersed in water on alumina substrates (٨mm×٤mm) with Pt inter-digitized electrodes and a Pt heater located on the backside. The structure of the fabricated sensor device has been reported elsewhere [٢٢]. Before sensing tests, a thermal treatment at ٤٠٠ ◦C for ٢ h was carried out in order to stabilize the microstructure of the sensing film. The sensors were then introduced in a stainless-steel test chamber for the sensing tests. The experimental bench for the electrical characterization of the sensors allows carrying out measurements in controlled atmosphere. Gases coming from certified bottles can be further diluted in air at a given concentration by mass flow controllers. Sensing measurements were carried out in the temperature range from ١٥٠ to ٤٠٠ ◦C, with steps of ٥٠ ◦C, under a dry air total stream of ٢٠٠ sccm, collecting the sensors resistance data in the four point mode. A multimeter data acquisition unit Agilent ٣٤٩٧٠A was used for this purpose, while a dual-channel power supplier instrument Agilent E٣٦٣٢A was employed to bias the built-in heater of the sensor to perform measurements at super-ambient temperatures. The gas response is defined as the ratio R_{air}/R_{gas}, where R_{air} is the electrical resistance of the sensor in dry air and R_{gas} the resistance at different $CO_٢$ concentrations.

Results and discussion

Reaction of L= BDCA with a mixture of Sc(III) nitrate in methanol led to the formation of a new ٣D Sc(III) coordination polymer . Nanopowders of this Coordination-Polymer was obtained by ultrasonic irradiation in a methanolic solution. while single crystals of NCP were obtained using a heat gradient applied to a solution of the reagents (the "branched tube method"). Scheme ١ gives an overview of the methods used for the synthesis of CP and NCP using the two different routes.

$$Sc(NO_3)_3 + BDCA \rightarrow \begin{cases} \xrightarrow{(MeOH)\ in\ Branched-Tube} \{Single\ Crystal\ of\ [Sc(OH)(BDCA)]_n \\ \xrightarrow{Ultrasond\ Irradiation+(MeOH)} \{Nanoscale\ of\ [Sc(OH)(BDCA)]_n \rightarrow \\ \xrightarrow{Calcination\ at\ 500-600^\circ C} Nanoparticle\ of\ Sc_2O_3 \end{cases}$$

Structural Study

The elemental analysis and IR spectra of the nanopowders and of the single crystalline material are indistinguishable. The relatively weak IR absorption bands around ۳۰۲۰-۳۰۳۲ cm^{-1} are due to the C-H modes of the aromatic ring hydrogen atoms. The antisymmetric ν_{asym}(CdO) vibrations in the range ۱۵۷۰-۱۵۰۰ cm^{-1} and the symmetric ν_{sym}(CdO) vibrations at ۱۴۱۰ cm^{-1}. The difference between the bands ν_{asym}(COO^- = ۱۵۶۶ cm^{-1}) and ν_{sym}(COO^- = ۱۴۱۰ cm^{-1}) then $\Delta\nu$ = ۱۵۶ cm^{-1}) confirms the bridging mode of the carboxylate groups in this compound.

Single crystal X-ray diffraction analysis of the compound CP was carried out. The ORTEP diagrams and packing of the title complexes are shown in Figures. ۱a and ۱b. This compound is tree-dimensional neutral coordination polymer and consists of the Sc(III) ions bridged by BDCA ligands, thus forming a ۳D infinite framework.

CP $[Sc(OH)(BDCA)]_n$ Structure is composed of chains of octahedral scandium units which are joined together via bridging hydroxyl groups, forming Sc-OH-Sc chains parallel to the *a*-axis. The oxygen atoms of the BDCA groups occupy the equatorial positions of the scandium octahedral, allowing for the terephthalate linker to bridge the scandium chains, Figure. ۲a. allowing the formation of a three dimensional framework with relatively large pores running parallel to *a*, as shown in Figure. ۲b.

The cell parameters for the synthesized CP, listed in Table.۱. Shown that the *b*-axis, and consequently the width of the pore, is shorter for structure $[Sc(OH)(BDCA)]_n$ (۱۱,۰۹Å). The *a*-axis and consequently the long dimension of the pore being slightly longer, is slightly longer for structure $[Sc(OH)(BDCA)]_n$ (۱۸,۱۱Å) in comparison. These differences are predominantly due to the flexibility of the lattice via scissoring motions, rather than differences in the cationic radii between the different trivalent metal cations. The crystallographic information is outlined in Table. ۱. with atomic co-ordinates listed below in Table. ۲. It is instructive to compare the crystallographic parameters of structure CP in order to understand the effects which the scandium cation has upon the system.

Figure. ۳. Schematic representations of a single pore of the CP. Diameters have been shown, illustrating the breadth and depth of the pore, showing that the pore in structure CP is ۲Å shorter in height, and ۱Å wider than its other analogue.

Figure. ٤. shows the XRPD pattern of compound simulated from its single crystal X-ray data, the XRPD pattern of prepared by the sonochemical process. Acceptable matches were observed between the simulated and experimental powder X-ray diffraction patterns. This indicates that the compound obtained by sonochemical process has single crystalline phases, almost identical to that obtained by the branched tube method. The significant broadening of the peaks indicates that the particles are of nanometer dimensions. Estimated by the Sherrer formula, $D = ۰,۸۹۱\lambda/\beta\cos\theta$, where D is the average grain size, λ the X-ray wavelength (۰,۱۵٤۰۵ nm), and θ and β the diffraction angle and full-width at half maximum of an observed peak, respectively, the average size of the particles is ۵۰ nm, which is in agreement with that observed by scanning electron microscopy, as shown in Figure. ۳. The morphology of the compound

prepared sonochemical method is the same and they are composed of particles with sizes of about ٤٠ nm. As can be seen from Figure. ٤. the comparison of the experimental and simulated PXRD patterns shows that there are two phases present in the product; CP and NCP is the minor product and the major product unfortunately could not be identified. Estimated by the Sherrer formula, $D = ٠,٨٩١\lambda/\beta\cos\theta$, where D is the average grain size, λ the X-ray wavelength (٠,١٥٤٠٥ nm), and θ and β the diffraction angle and full-width at half maximum of an observed peak, respectively, the average size of the particles is ٥٠ nm, which is in agreement with that observed by scanning electron microscopy, as shown in Figure. ٥. The morphology of the compound prepared sonochemical method (Figure. ٥.) is the same and they are composed of particles with sizes of about ٤٠ nm.

To examine the thermal stability of the nanopowders and the single crystals of this CP and NCP, thermal analyses (TGA-DTA) were carried out between ٣٠ and ٨٠٠ °C in a static atmosphere of argon (Figures.٦a and ٦b). The compound as a bulk phase is very stable and does not decompose up to temperature of ٢٧٠ ºC, at which temperature decomposition starts. Between ٢٦٠ and ٣٥٠ ºC, removal of BDCA occurs with a mass loss of ٧٢,٩٪ (calculated ٧٦,٥٠٪). At higher temperatures, the residue, was decomposed and mass loss calculations show that the final decomposition product is $Sc_٢O_٣$ (Figure. ٦a.). Compared to the bulk material, nano-sized particles of the compound are much less stable and start to decompose at ٨٠ ºC. The TGA curve (Figure. ٦b) exhibits two distinct decomposition stages between ٨٠-٥٩٠ ºC with a total mass loss of ٧٦,٥٣٪ (calculated ٧١,٤٢٪). Detectable decomposition of the nanopowders begins about ١٠٠ ºC earlier than that of its bulk counterparts, probably due to the much higher surface to volume ratio of the nano-sized particles. Moreover, the DTA curves display an endothermic peak at ٣٥٠ ºC and one distinct exothermic peaks at ٤١٠ ºC for the single crystals of compound (Figure. ٦a), whereas only an wide endothermic peak at ٤٢٥-٥١٢ ºC for the nanopowders of this compound (Figure. ٦b). Both TGA and DTA results indicate that although both nano-sized and bulk materials have the same composition, they exhibit a different thermal decomposition behavior.

Thermal decomposition of the nanopowders of This Nano-Coordination-Polymer in air produced $Sc_٢O_٣$ nanopowders, respectively, as established by their powder XRPD patterns (Figure. ٧.). the obtained patterns match with the standard patterns of orthorhombic $Sc_٢O_٣$. The phase purity of the prepared tetragonal $Sc_٢O_٣$ nanopowders are completely obvious and all diffraction peaks are perfectly indexed to the tetragonal $Sc_٢O_٣$ structures. The broadening of the peaks indicated that the particles were of nanometer size and estimation by the Sherrer formula, $D = ٠,٨٩١\lambda/\beta\cos\theta$, shows that the average sizes of the particles are ٦٠ nm for $Sc_٢O_٣$ nanopowders, respectively (See Figure. ٧.).

Figures. ٨. shows the SEM images of the $Sc_٢O_٣$ nanopowders obtained from calcinations of the compound under laboratory atomsphere, respectively. The morphology of the nanoparticles of $Sc_٢O_٣$ is very similar to that of the compound (see Figures. ٥.). This point may be due to the direct removal of the L ligand without changing of morphology under the calcinations in air.

$CO_٢$ sensing tests

It is well known that the response of resistive sensors is highly affected by the operating temperature. Therefore, the response of the $Sc_٢O_٣$ sensors as a function of the operating temperature was first investigated. Figure. ٩. shows the response as a function of operating temperature from ١٥٠ to ٤٠٠ °C for the NCP sensor exposed to ٤٠٠ ppm of $CO_٢$. A rapid increase of the response was observed as the working temperature was increased and reached a maximum at about ٣٠٠ °C and started decreasing thereafter. This characteristic volcano curve can be interpreted on the basis of adsorption-desorption and reaction processes occurring on the sensing layer surface. For operating temperatures <٢٠٠ °C the sensor

response is low because the adsorbed $CO_۲$ molecules are not activated enough to react with the surface adsorbed oxygen species. However, above ۳۰۰ °C the decrease in $CO_۲$ gas adsorption is not adequately compensated by the increase of surface reaction and the sensor response decreases. The transient response was found reversible (Figure. ۱۰). The response time, τ_{res}, defined here as the time required to achieve ۹٤٪ of the total resistance change when $CO_۲$ is introduced into air, is fast (τ_{res}~ ۲۵ s). A slower recovery time, τ_{rec}, i.e. the time required to achieve ۹٤٪ of the total resistance change when $CO_۲$ is turned off and pure dry air is reintroduced into the chamber, has been observed (τ_{res}~ ۱۵۰ s). The response as a function of $CO_۲$ gas concentration for all the $Sc_۲O_۳$ sensors investigated at ۳۰۰ °C is shown in Figure. ۱۱. The sensors show a good response to $CO_۲$. The response increased as the $CO_۲$ gas concentration was increased from ۱۰۰ to ۵۰۰ ppm. Figure. ۱۲(NCP and $Sc_۲O_۳$). shows the sensor responses vs. $CO_۲$ concentration. A linear trend was observed, when responses are plotted in a log-log scale, as a function of the gas concentration. It is interesting to observe that all the nanostructured films display the same sensitivity to $CO_۲$ (SCO) as calculated by the slope of the extrapolated straight lines reporting the response as a function of the $CO_۲$ concentration in Figure. ۱۰b. the sensitivity with respect to $CO_۲$ was calculated to be ۰,۰۹۱ $ppm^{-۱}$. Instead, the responses at a given $CO_۲$ concentration and the detection limits, DL, defined as the lower concentration in which the response significantly differentiated from the noise signal, i.e. ۵ times the standard deviation of noise (instrumental detection limit), are different among the investigated sensors. NCP sensor, exhibits a slightly greater response than other sensor particles, while on $Sc_۲O_۳$ sensor nanopowders the lower response was found, and the same trend was found for the detection limits. The extrapolated limit of detection for the NCP sensor is about ۰,۸۵ ppm, allowing a monitoring of $CO_۲$ down to concentrations in the sub-ppm range. Even though a direct comparison with recent literature reports on $CO_۲$ sensing of various $Sc_۲O_۳$ nanostructures cannot be made because of the different experimental conditions adopted the results we obtained clearly indicate the good performances of our sensors.

Conclusion

A new Sc(III) Coordination Polymer, $[Sc(OH)(BDCA)]_n$ has been synthesized at single crystal by using a BT (Branched Tube) method and nanopowders by ultrasound irradiation (Sonochemistry Method). The compound was structurally characterized by single-crystal X-Ray Diffraction. The crystal structure of the compound consists of a ۳D coordination polymer in which the Sc(III) ions is octahedral coordinated by BDCA ligands. TGA studies indicate that reduction of the particle size of the coordination polymers of to a few dozen nanometers results in lower thermal stability when compared to the single crystalline samples. The calcinations of this compound under air atmospheres produce $Sc_۲O_۳$ nanopowders. This study demonstrates the coordination polymers may be suitable precursors for the respectively and simple preparation of nanoscale. These nanostructures were investigated in the monitoring of carbon-dioxide, showing the maximum of response around ۳۰۰ °C. The higher response was obtained for the NCP sensor based on $Sc_۲O_۳$ nanoparticles. A synergic effect between small crystallite size/high surface area and potential barrier modification is proposed for explaining the enhanced sensing properties of the $Sc_۲O_۳$ particles. In summary, from this study, it can be deduced that the performance of resistive NCP based sensors to $CO_۲$ gas can be controlled by tuning the nanoparticles of coordination polymers by a rapid synthesis procedure assisted by BT and sonochemical, providing a simple way to fabricate highly sensitive $CO_۲$ gas sensors.

Supplementary data

CCDC ۹۸۵٤٥٤ contains the supplementary crystallographic data for $[Sc(OH)(BDCA)]_n$. These data can be obtained free of charge via http://www.ccdc.cam.ac.uk/conts/retrieving.html, or from the Cambridge Crystallographic Data Centre, ۱۲ Union Road, Cambridge CB۲ ۱EZ, UK; fax: (+٤٤) ۱۲۲۳-۳۳٦-۰۳۳; or e-mail: deposit@ccdc.cam.ac.uk.

Acknowledgements

This work Proffer to Prof. Dr. Veysel Turan YILMAZ. Supporting of this investigation by the Lorestan University, Khorram Abad, Lorestan, Islamic Republic of Iran and Ataturk University of Erzurum, Turkey, is gratefully acknowledged.

References

[۱] J. C. Bailar, Preparative Inorganic Reaction. Vol۱, Interscience, York, ۱۹٦٤.
[۲] C. Janiak. Dalton Trans, (۲۰۰۳) ۲۷۸۱.
[۳] C.B. Murray, C.R. Kagan, M.G. Bawendi, Annu. Rev. Matter Sci. ۳۰ (۲۰۰٦) ٥٤٥.
[٤] G.-M. Chow, N. IvanovaNoskova, Nano-structured Materials Science and Technology, Kluwer Academic publishers, Dordrecht, ۱۹۹۸.
[٥] L. Mazzola, Nat. Biotechnol. ۲۱ (۲۰۰۳) ۱۱۳۷.
[٦] R. Paul, J. Wolfe, P. Hebert, M. Sinkula, Nat. Biotechnol. ۲۰ (۲۰۰۳) ۲۷۷.
[۷] G. Blaser, T. Ruhl, C. Diehl, M. Ulrich, D. Kohl, Physica A: Statistical and Theoretical Physics ۲٦٦ (۱۹۹۹) ۲۱۸–۲۲۳.
[۸] G. Korotcenkov, Sensors and Actuators B ۱۰۷ (۲۰۰٥) ۲۰۹–۲۳۲.
[۹] B. Levy, Journal of Electroceramics ۱ (۱۹۹۷) ۲۳۹–۲۷۲.
[۱۰] J. Bandara, C.M. Divarathne, S.D. Nanayakkara, Solar Energy Materials and Solar Cells ۸۱ (۲۰۰٤) ٤۲۹–٤۳۷.
[۱۱] J. Bandara, J.P. Yasomanee, Semiconductor Science and Technology ۲۲ (۲۰۰۷) ۲۰–۲٤.
[۱۲] C.L. Liao, Y.H. Lee, S.T. Chang, K.Z. Fung, Journal of Power Sources ۱٥۸ (۲۰۰٦) ۱۳۷۹–۱۳۸٥.
[۱۳] Sang Sub Kim, Han Gil Na, Sun-Woo Choi, Dong Sub Kwak, Hyoun Woo Kim, Microelectronic Engineering, ۱۰٥, ۲۰۱۳, ۱-۷.
[۱٤] M. Faisal, Sher Bahadar Khan, Mohammed M. Rahman, Aslam Jamal, M.M. Abdullah, Applied Surface Science, ۲٥۸, ۱۹, ۲۰۱۲, ۷٥۱٥-۷٥۲۲.
[۱٥] Babita Baruwati, D. Kishore Kumar, Sunkara V. Manorama, Sensors and Actuators B: Chemical, ۱۱۹, ۲, ۲۰۰٦, ٦۷٦-٦۸۲.
[۱٦] Prabhakar Rai, Yeon-Tae Yu, Sensors and Actuators B: Chemical, ۱۷۳, ۲۰۱۲, ٥۸-٦٥.
[۱۷] Y.T. Wang, L. Yu, J. Wang, L. Lou, W.J. Du, Z.Q. Zhu, H. Peng, J.Z. Zhu, , Journal of Electroanalytical Chemistry, ٦٦۱, ۱, ۲۰۱۱, ۸-۱۲.
[۱۸] M.C. Carotta, A. Cervi, V. di Natale, S. Gherardi, A. Giberti, V. Guidi, D. Puzzovio, B. Vendemiati, G. Martinelli, M. Sacerdoti, D. Calestani, A. Zappettini, M. Zha, L. Zanotti, Sensors and Actuators B: Chemical, ۱۳۷, ۱, ۲۰۰۹, ۱٦٤-۱٦۹.
[۱۹] Geyu Lu, Jing Xu, Jianbo Sun, Yingshuo Yu, Yiqun Zhang, Fengmin Liu, Sensors and Actuators B: Chemical, ۱٦۲, ۱, ۲۰۱۲, ۸۲-۸۸.
[۲۰] Rigaku/MSC, Inc., ۹۰۰۹ new Trails Drive, The Woodlands, TX ۷۷۳۸۱.
[۲۱] Sheldrick, G. M., SHELXS۹۷ and SHELXL۹۷, University of Göttingen, Germany, ۱۹۹۷.

[۲۲] Alireza Aslani, Physica B: Condensed Matter, ٤٠٦, ۲, ۲۰۱۱, ۱٥۰-۱٥٤.

Figure. ۱. (a) Labeled atoms in compound CP $[Sc(OH)(BDCA)]_n$, (b) a fragment of the ۳D polymer in compound.

Figure. ۲. (۲a and ۲b) Projection down [۰۰۱] of structure CP showing chains of scandium octahedral, joined by hydroxyl groups.

Table. ۱. X-Ray Crystallography datas from the structural determination of CP $[Sc(OH)(BDCA)]_n$.

Table. ۲. Atomic Coordinated for $[Sc(OH)(BDCA)]_n$.

Figure. ۳. Schematic representations of a single pore of the single pore from structure CP ($[Sc(OH)(BDCA)]_n$).

Figure. ٤. The XRPD patterns ۱:(a) simulated from single crystal X-ray data of compound (CP), (b) nano-structured of compound prepared by the sonochemical method (NCP) and (c) prepared by colorless single crystals of $[Sc(OH)(BDCA)]_n$ (CP).

Figure. ٥. SEM image of nanopowders of compound (NCP) $[Sc(OH)(BDCA)]_n$, produced by sonochemical method.

Figure. ٦a. TGA curves of **CP**: (**a**) single crystals and (**b**) asnanopowders.

Figure. ٦b. DTA curves of **CP**: (**a**) as single crystals (CP) and (**b**) as nanopowders (NCP).

Figure. ۷. XRPD patterns of $Sc_۲O_۳$ nanopowders, prepared by calcinations of compound NCP (nano coordination polymer).

Figure. ۸. SEM photograph of $Sc_۲O_۳$ nanopowders produced by calcination of compound NCP (nano coordination polymer**)** at laboratory atmosphere.

Figure. ۹. Response to ٤۰۰ ppm of $CO_۲$ vs. the operating temperature of the NCP sensor.

Figure. ۱۰. Transient response of NCP sensor to exposure of ۱۰۰ ppm of $CO_۲$ at ۳۰۰ °C.

Figure. ۱۱. Response to different $CO_۲$ gas concentration for the $Sc_۲O_۳$ sensors at ۳۰۰ °C.

Figure. ۱۲. (a) Calibration curves of the $Sc_۲O_۳$ sensors at ۳۰۰ °C; (b) calibration curves of the $Sc_۲O_۳$ sensors showing the measured sensitivity to $CO_۲$ and the extrapolated detection limit related to NCP sensor.

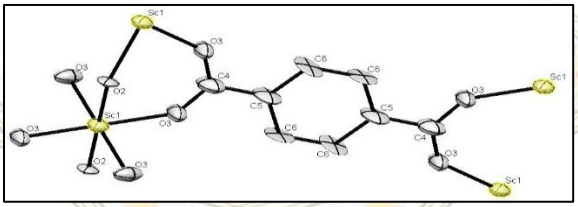

(۱a)

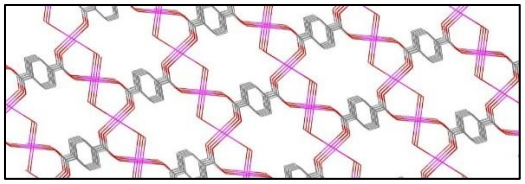

(۱b)

Figure. ۱. (a) Labeled atoms in compound CP $[Sc(OH)(BDCA)]_n$, (b) a fragment of the ۳D polymer in compound.

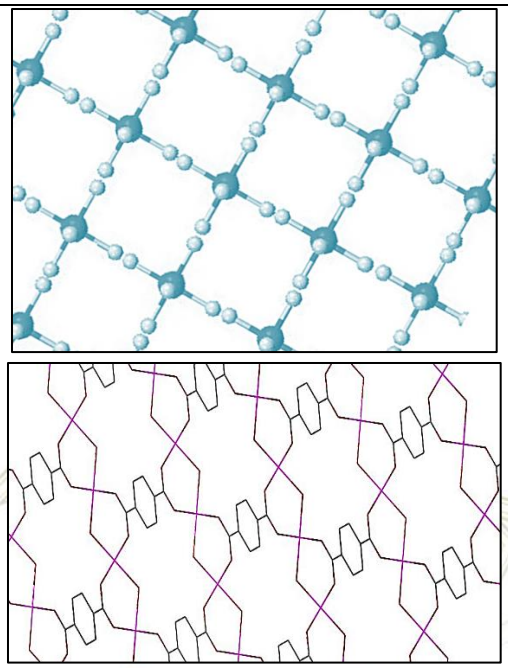

Figure. ۲. (۲a and ۲b) Projection down [۰۰۱] of structure CP showing chains of scandium octahedral, joined by hydroxyl groups.

Table. ۱. X-Ray Crystallography datas from the structural determination of CP $[Sc(OH)(BDCA)]_n$.

Identification code	۹۷۵۱۹٤
Empirical formula	$Sc(OH)(C_۸H_۶O_۴)$
Formula weight	۲۲۵,۰۷
Temperature	۲۹۳(۲) K
Wavelength	۰,۷۱۰۳ Å
Crystal system	Orthorombic
space group	Imcm
Unit cell dimensions	a=۱۸,۱۱۲(۱۵) Å
	b= ۱۱,۵۹۰(۲۵) Å
	c= ۷,۲۲۵(۳۹) Å
	α = ۹۰
	β = ۹۰
	γ = ۹۰
Volume	۱۵۱٦,۷(۸۹) $Å^۳$
Z	۱٦
Calculated density	۱,۳۱۱ g $cm^{-۱}$
Theta range for data collection	۲,۰۹ to ۲۵,٦۵ deg
Reflections collected/unique	۵۰۹۳/۸۰۷
Completeness to theta= ۲۷,۳۸	۹۷,٤ %
$R۱(I > ۲\sigma(I)$, $wR۲$ (All data)	۰,۲۳۳٤, ۰,۲۷۰۷

Table. ۲. Atomic Coordinated for $[Sc(OH)(BDCA)]_n$.

Atoms	X	Y	Z	U_{iso}	O_{cc}	Multiplicity
Sc(۱)	۰,۷۵	۰,۲۵	۰,۲۵	۰۲,۰۲۹۹(۱٦)	۱	٤
O(۱)	۰,٦٦۹٦(۱۳)	۰,۳٦۰۸(۹)	۰,۱٤۹٥(٥)	۰,۰۳۰(٤)	۱	۱
O(۲)	۰,۷٥	۰,۱٦٤۹(۱٥)	۰	۰,۰۳۰(٤)	۱	٤
C(۱)	۰,٥۳۸۷(۲)	۰,٤۷۱٥(۱۷)	۰,۱٥۷۷(۸)	۰,۰٤۹(۸)	۱	۱
C(۲)	۰,٦۳۸۸(۲)	۰,۳۸۳٤(۱۳)	۰	۰,۰٦۲(۷)	۱	۲
C(۳)	۰,٥٦۸٤(۲)	۰,٤٤۹٦(۱٥)	۰	۰,۰۷۳(٦)	۱	۲

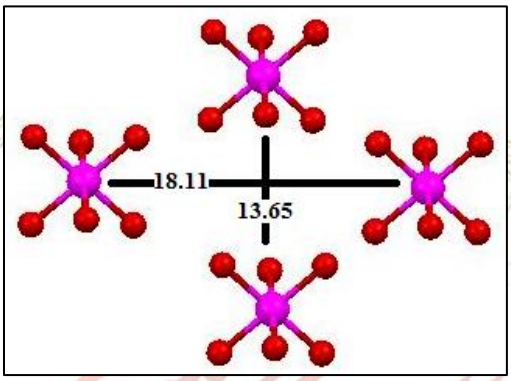

Figure. ۳. Schematic representations of a single pore of the single pore from structure CP ($[Sc(OH)(BDCA)]_n$).

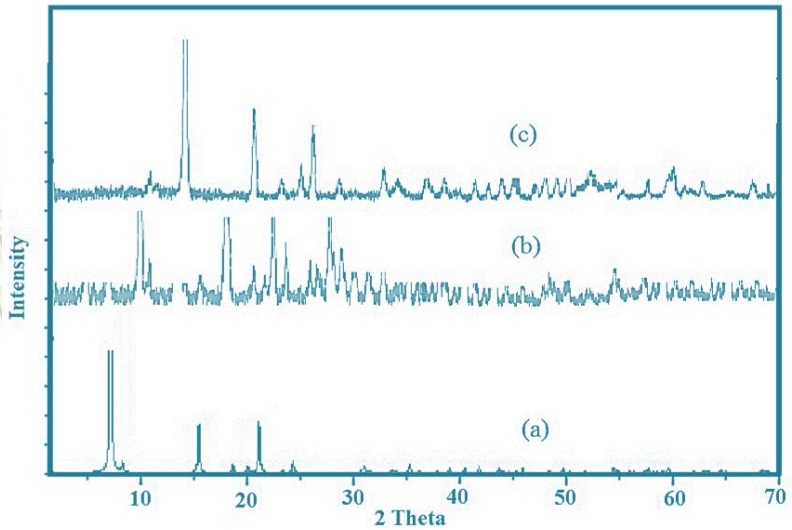

Figure. ٤. The XRPD patterns ۱:(a) simulated from single crystal X-ray data of compound (CP), (b) nano-structured of compound prepared by the sonochemical method (NCP) and (c) prepared by colorless single crystals of $[Sc(OH)(BDCA)]_n$ (CP).

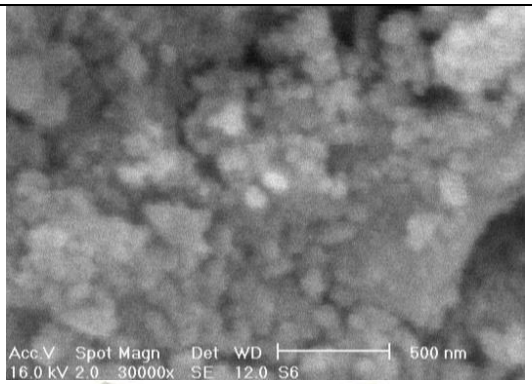

Figure. ٥. SEM image of nanopowders of compound (NCP) $[Sc(OH)(BDCA)]_n$, produced by sonochemical method.

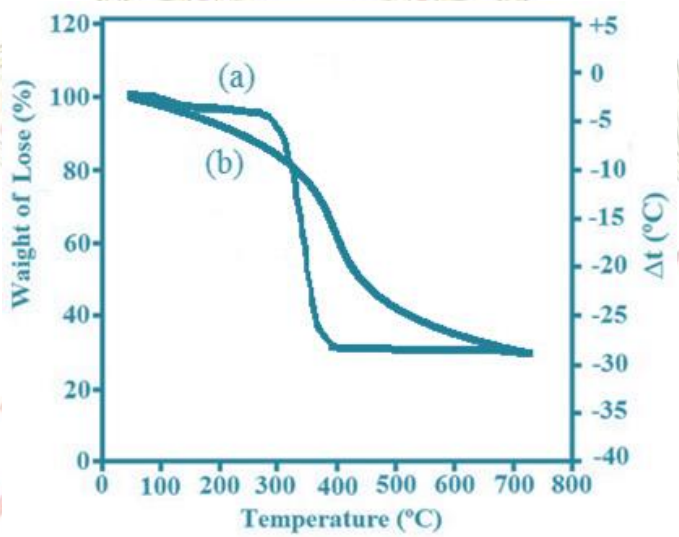

Figure. ٦a. TGA curves of **CP**: (**a**) single crystals and (**b**) asnanopowders.

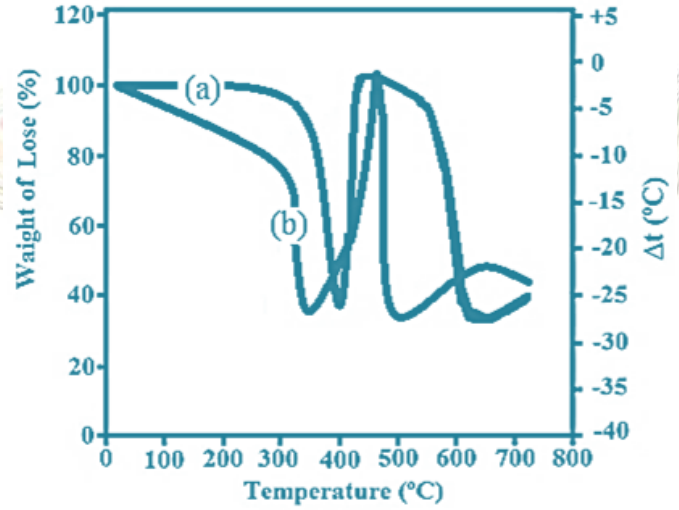

Figure. ٦b. DTA curves of **CP**: (**a**) as single crystals (CP) and (**b**) as nanopowders (NCP).

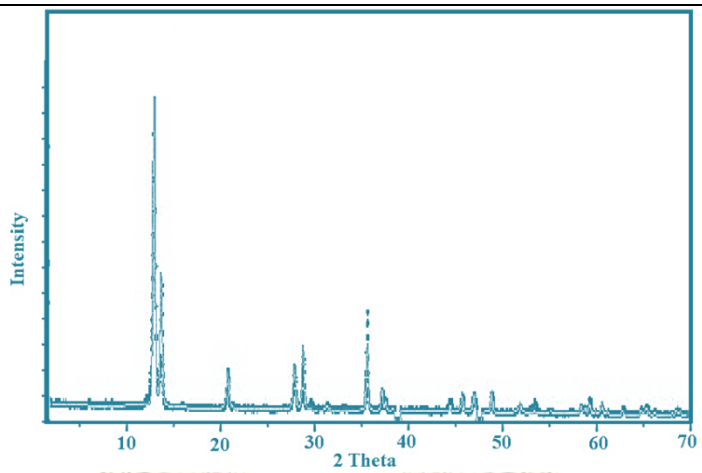

Figure. ۷. XRPD patterns of Sc_2O_3 nanopowders, prepared by calcinations of compound NCP (nano coordination polymer).

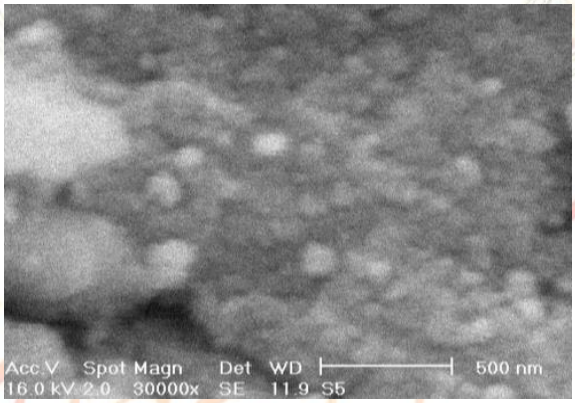

Figure. ۸. SEM photograph of Sc_2O_3 nanopowders produced by calcination of compound NCP (nano coordination polymer**)** at laboratory atmosphere.

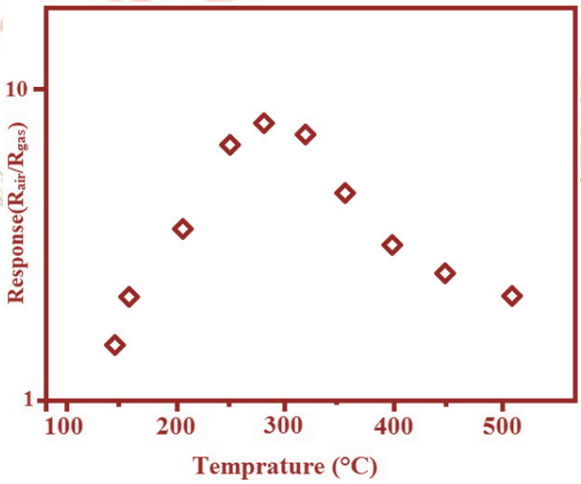

Figure. ۹. Response to ٤٠٠ ppm of CO_2 vs. the operating temperature of the NCP sensor.

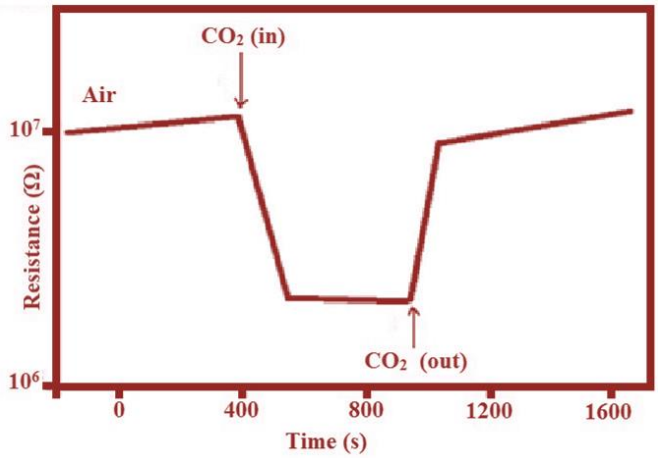

Figure. ۱۰. Transient response of NCP sensor to exposure of ۱۰۰ ppm of CO_2 at ۳۰۰ °C.

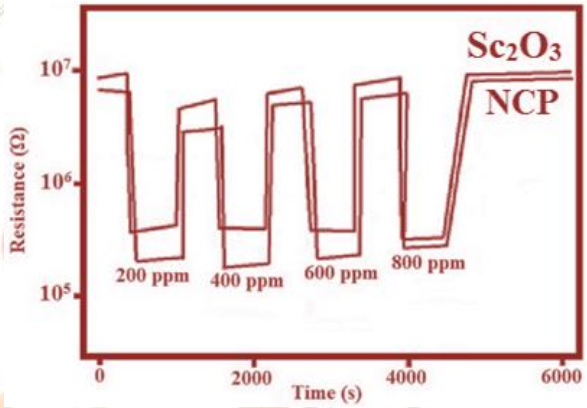

Figure. ۱۱. Response to different CO_2 gas concentration for the Sc_2O_3 sensors at ۳۰۰ °C.

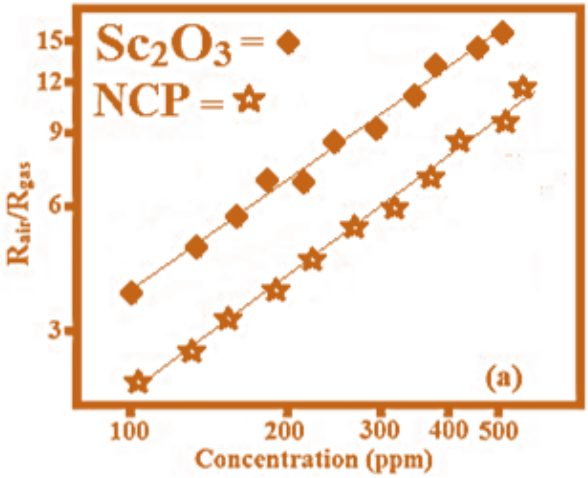

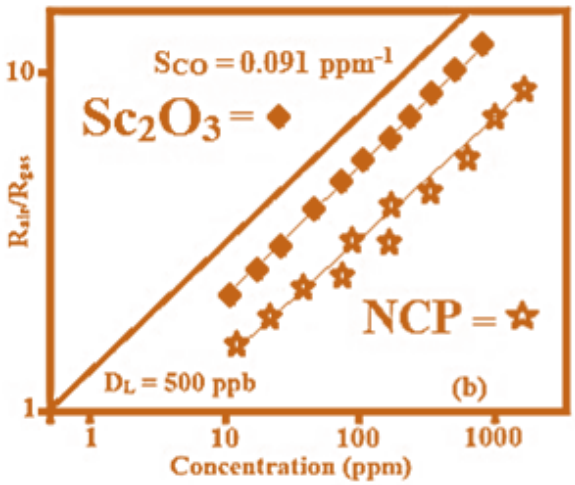

Figure. ۱۲. (a) Calibration curves of the Sc_2O_3 sensors at ۳۰۰ °C; (b) calibration curves of the Sc_2O_3 sensors showing the measured sensitivity to CO_2 and the extrapolated detection limit related to NCP sensor.